High resolution spectroscopic study of 10Be-Λ

(HKS(JLab E05-115) Collaboration) Gogami, T.; ...; Androić, Darko; ...; Furić, Miroslav; ...; Petković, Tomislav; ...; Ševa, Tomislav; ...; ...

PHYSICAL REVIEW C **93**, 034314 (2016)

High resolution spectroscopic study of $^{10}_{\Lambda}$Be

T. Gogami,[1,*] C. Chen,[2] D. Kawama,[1] P. Achenbach,[3] A. Ahmidouch,[4] I. Albayrak,[2] D. Androic,[5] A. Asaturyan,[6] R. Asaturyan,[6,†] O. Ates,[2] P. Baturin,[7] R. Badui,[7] W. Boeglin,[7] J. Bono,[7] E. Brash,[8] P. Carter,[8] A. Chiba,[1] E. Christy,[2] S. Danagoulian,[4] R. De Leo,[9] D. Doi,[1] M. Elaasar,[10] R. Ent,[11] Y. Fujii,[1] M. Fujita,[1] M. Furic,[5] M. Gabrielyan,[7] L. Gan,[12] F. Garibaldi,[13] D. Gaskell,[11] A. Gasparian,[4] Y. Han,[2] O. Hashimoto,[1,‡] T. Horn,[11] B. Hu,[14] Ed. V. Hungerford,[15] M. Jones,[11] H. Kanda,[1] M. Kaneta,[1] S. Kato,[16] M. Kawai,[1] H. Khanal,[7] M. Kohl,[2] A. Liyanage,[2] W. Luo,[14] K. Maeda,[1] A. Margaryan,[6] P. Markowitz,[7] T. Maruta,[1] A. Matsumura,[1] V. Maxwell,[7] A. Mkrtchyan,[6] H. Mkrtchyan,[6] S. Nagao,[1] S. N. Nakamura,[1] A. Narayan,[17] C. Neville,[7] G. Niculescu,[18] M. I. Niculescu,[18] A. Nunez,[7] Nuruzzaman,[17] Y. Okayasu,[1] T. Petkovic,[5] J. Pochodzalla,[3] X. Qiu,[14] J. Reinhold,[7] V. M. Rodriguez,[19] C. Samanta,[20] B. Sawatzky,[11] T. Seva,[5] A. Shichijo,[1] V. Tadevosyan,[6] L. Tang,[2,11] N. Taniya,[1] K. Tsukada,[1] M. Veilleux,[8] W. Vulcan,[11] F. R. Wesselmann,[21] S. A. Wood,[11] T. Yamamoto,[1] L. Ya,[2] Z. Ye,[2] K. Yokota,[1] L. Yuan,[2] S. Zhamkochyan,[6] and L. Zhu[2]

(HKS(JLab E05-115) Collaboration)

[1]*Department of Physics, Graduate School of Science, Tohoku University, Sendai, Miyagi 980-8578, Japan*

[2]*Department of Physics, Hampton University, Hampton, Virginia 23668, USA*

[3]*Institute for Nuclear Physics, Johannes Gutenberg-University, D-55099 Mainz, Germany*

[4]*Department of Physics, North Carolina A&T State University, Greensboro, North Carolina 27411, USA*

[5]*Department of Physics & Department of Applied Physics, University of Zagreb, HR-10000 Zagreb, Croatia*

[6]*A.I. Alikhanyan National Science Laboratory, Yerevan 0036, Armenia*

[7]*Department of Physics, Florida International University, Miami, Florida 27411, USA*

[8]*Department of Physics, Computer Science & Engineering, Christopher Newport University, Newport News, Virginia 23606, USA*

[9]*Istituto Nazionale di Fisica Nucleare, Sezione di Bari and University of Bari, I-70126 Bari, Italy*

[10]*Department of Physics, Southern University at New Orleans, New Orleans, Louisiana 70126, USA*

[11]*Thomas Jefferson National Accelerator Facility (JLab), Newport News, Virginia 23606, USA*

[12]*Department of Physics, University of North Carolina at Wilmington, Wilmington, North Carolina 28403, USA*

[13]*INFN, Sezione Sanità and Istituto Superiore di Sanità, 00161 Rome, Italy*

[14]*Nuclear Physics Institute, Lanzhou University, Lanzhou, Gansu 730000, China*

[15]*Department of Physics, University of Houston, Houston, Texas 77204, USA*

[16]*Department of Physics, Yamagata University, Yamagata, 990-8560, Japan*

[17]*Mississippi State University, Mississippi State, Mississippi 39762, USA*

[18]*Department of Physics and Astronomy, James Madison University, Harrisonburg, Virginia 22807, USA*

[19]*Escuela de Ciencias y Tecnologia, Universidad Metropolitana, San Juan, 00928, Puerto Rico*

[20]*Department of Physics & Astronomy, Virginia Military Institute, Lexington, Virginia 24450, USA*

[21]*Department of Physics, Xavier University of Louisiana, New Orleans, Louisiana 70125, USA*

(Received 16 November 2015; revised manuscript received 7 January 2016; published 10 March 2016)

Spectroscopy of a $^{10}_{\Lambda}$Be hypernucleus was carried out at JLab Hall C using the $(e,e'K^+)$ reaction. A new magnetic spectrometer system (SPL+HES+HKS), specifically designed for high resolution hypernuclear spectroscopy, was used to obtain an energy spectrum with a resolution of ∼0.78 MeV (FWHM). The well-calibrated spectrometer system of the present experiment using $p(e,e'K^+)\Lambda$, Σ^0 reactions allowed us to determine the energy levels; and the binding energy of the ground-state peak (mixture of 1^- and 2^- states) was found to be $B_\Lambda = 8.55 \pm 0.07(\text{stat.}) \pm 0.11(\text{sys.})$ MeV. The result indicates that the ground-state energy is shallower than that of an emulsion study by about 0.5 MeV which provides valuable experimental information on the charge symmetry breaking effect in the ΛN interaction.

DOI: 10.1103/PhysRevC.93.034314

I. INTRODUCTION

Knowledge of the nucleon-nucleon (NN) system can be generalized to the baryon-baryon (BB) system using SU(3) flavor symmetry. A study of the hyperon-nucleon (YN) system is a natural extension as a first step from NN to BB systems. However, a YN scattering experiment, which is the most straightforward way to explore the interaction, is very limited due to the short lifetimes of hyperons (e.g., $\tau = 263$ ps for Λ). Thus, there has been interest in hyperon binding in a nucleus where the YN interaction can be studied with higher precision and greater statistical accuracy. The spectroscopy of Λ hypernuclei was begun approximately 60 years ago following the serendipitous discovery of a hypernucleus in an emulsion exposed to cosmic rays [1] to investigate the ΛN interaction. Counter experiments initially used either

[*]Current address: Department of Physics, Kyoto University, Kyoto, 606-8502, Japan.

[†]Deceased.

[‡]Deceased.

the (K^-,π^-) and (π^+,K^+) reactions in facilities located in CERN, BNL, and KEK. A number of Λ hypernuclei have been observed up to a nuclear mass of $A = 209$, and new features which do not present in the ordinary nuclear system were observed in the hypernuclear system [2]. One of the most novel results from the hypernuclear spectroscopy is the clear evidence of nuclear shell structures even for deep orbital states in heavy mass nuclei, measured by the (π^+,K^+) experiments [2]. This is thanks to a fact that a single embedded Λ is not excluded from occupying inner nuclear shells by the Pauli principle from nucleons. Thus, the Λ can dynamically probe the nuclear interior as an impurity. However, more accurate and detailed structures for a variety of hypernuclei are still needed to improve our understanding of the strongly interacting system with a strangeness degree of freedom, and today researchers are attempting to measure them in complementary ways at J-PARC using hadron beams [3], GSI (FAIR) using heavy ion beams [4], and MAMI [5] and JLab using electron beams [7–14].

II. MISSING MASS SPECTROSCOPY OF Λ HYPERNUCLEI WITH ELECTRON BEAMS

Missing mass spectroscopy using the $(e,e'K^+)$ reaction started in 2000 at Thomas Jefferson National Accelerator Facility (JLab) [7,8]. The missing mass spectroscopy with primary electron beams enabled us to have better energy resolution in the resulting hypernuclear structure than that with currently available hadron beams (FWHM of a few MeV). These initial studies demonstrated that FWHM $\simeq$0.9 MeV resolution was possible. Then, experiments at JLab in 2005 and 2009 (JLab E01-011 [12–14] and E05-115 [14]) were performed with new magnetic spectrometers specifically designed for a resolution of FWHM $\simeq$0.5 MeV which is the best in the missing mass spectroscopy of the Λ hypernuclei. In terms of energy resolution, γ-ray spectroscopy [2], which measures deexcitation γ rays from hypernuclei, is better (typically FWHM $\simeq$ a few keV) than that of the missing mass spectroscopy. Λ hypernuclei with the light mass numbers ($A \leqslant 19$) were investigated by γ-ray spectroscopy with such a high energy resolution up to now. However, it measures only energy-level spacing and cannot give absolute binding energy and production cross section information. Therefore, missing mass measurements and γ-ray spectroscopy are complementary, and both of them are important.

In addition to providing higher resolution in the missing mass spectroscopy, the $(e,e'K^+)$ reaction has other useful features. An absolute mass scale can be calibrated with the $p(e,e'K^+)\Lambda$, Σ^0 reactions, since all masses are known [15], and in particular, the reaction constituents lead to clearly resolved peaks which are well separated from backgrounds. Furthermore, the $(e,e'K^+)$ reaction converts a nuclear proton into a Λ in contrast to mesonic reactions which convert a neutron into a Λ. Comparison of these isotopic mirror hypernuclei provides information on hypernuclear charge symmetry. This paper reports the first result of a spectroscopic measurement of ${}^{10}_{\Lambda}$Be with the new spectrometers that allowed us to observe the finer nuclear structures and to determine the energy levels with a better precision than those of the previous Λ hypernuclear missing mass spectroscopy.

III. MOTIVATION FOR THE MEASUREMENT OF ${}^{10}_{\Lambda}$Be

The present study compares the ground-state binding energies of ${}^{10}_{\Lambda}$Be $(\alpha+\alpha+n+\Lambda)$ to that of its isotopic mirror nucleus ${}^{10}_{\Lambda}$B $(\alpha+\alpha+p+\Lambda)$, providing information on the mechanism of charge symmetry breaking (CSB) in hypernuclei. The most evident fact of the ΛN CSB is the ground-state binding energy difference of $A = 4$ iso-doublet $(T = 1/2)$ hypernuclei, $B_\Lambda({}^4_\Lambda\mathrm{He}) - B_\Lambda({}^4_\Lambda\mathrm{H}) = (2.39 \pm 0.03) - (2.04 \pm 0.04) = +0.35 \pm 0.06$ MeV [16]. The Λ's binding energy is defined by using masses of Λ (M_Λ) and the core nucleus, for example, $B_\Lambda({}^4_\Lambda\mathrm{He}) = M({}^3\mathrm{He}) + M_\Lambda - M({}^4_\Lambda\mathrm{He})$. The binding energy difference is larger than our expectation even after a correction in the change in the Coulomb energy due to core contraction, and it is attributed to the ΛN CSB effect [17,18]. Many theorists have tried to understand the origin of the ΛN CSB for more than 40 years [17–23], but it still has not been fully understood. Recently, the binding energy of ${}^4_\Lambda$H was remeasured by decayed pion spectroscopy at MAMI to confirm the emulsion measurement [5]. The result of $B_\Lambda({}^4_\Lambda\mathrm{H}) = 2.12 \pm 0.01 \pm 0.09$ MeV is consistent with that of the emulsion experiment. Results from a recent γ-ray spectroscopy measurement indicated that the CSB effect of 1^+ states in the $A = 4$, $T = 1/2$ hypernuclear system is small, which demonstrated that the CSB interaction strongly depends on the spin [6]. The study of the ΛN CSB effect in a p-shell hypernuclear system is also in the spotlight these days [13,19,21,23]. A study for the $A = 7$, $T = 1$ Λ hypernuclei, which are one of the simplest p-shell systems, showed that the experimental results [13] do not favor a phenomenological ΛN CSB potential in the cluster model [21]. A similar study in $A = 10$, $T = 1/2$ system was performed by comparing the ground-state binding energies of ${}^{10}_{\Lambda}$Be and ${}^{10}_{\Lambda}$B [19,23]. However, the reported binding energy of ${}^{10}_{\Lambda}$Be was a weighted-mean value of only three events measured in the emulsion experiment [24,25] though the binding energy of ${}^{10}_{\Lambda}$B was determined by higher statistics (nevertheless there are only ten events). Thus, the binding energy measurement of ${}^{10}_{\Lambda}$Be with higher statistics and a smaller systematic error has been awaited and is necessary, using an independent way from the emulsion study.

Additionally, the Λ binding energy and low-lying structure of ${}^{10}_{\Lambda}$Be are also relevant to a study of the ΞN interaction on which there is almost no experimental information so far. An event of a bound system of Ξ^--^{14}N decaying into ${}^{10}_{\Lambda}$Be and ${}^{5}_{\Lambda}$He was recently identified in an emulsion experiment at KEK [26]. The analysis of this event was done using theoretically predicted energy levels of ${}^{10}_{\Lambda}$Be to obtain the Ξ^- binding energy. This present study provides the energy levels of ${}^{10}_{\Lambda}$Be experimentally for the first time.

IV. EXPERIMENTAL SETUP

The experiment was performed at JLab Hall C using continuous wave electron beams accelerated by CEBAF. Figure 1 shows the experimental geometry of JLab E05-115. Electrons with the energy of 2.344 GeV were incident on a

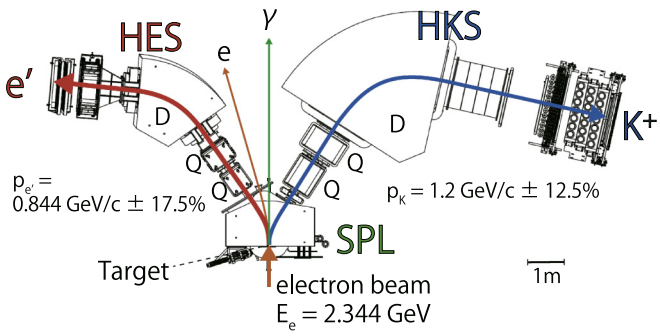

FIG. 1. A schematic drawing of the JLab E05-115 experimental geometry. The setup consists of SPL, HKS, and HES spectrometers. An electron beam with the energy of 2.344 GeV is incident on the target located at the entrance of SPL. A K^+ and an e' with the momenta of ~1 GeV/c are observed by HKS and HES, respectively.

target which was located at the entrance of a charge separation dipole magnet (SPL). Momentum vectors of the reaction K^+s ($p_K^{\rm center} = 1.200$ GeV/c) and the scattered electrons ($p_{e'}^{\rm center} = 0.844$ GeV/c) at the target were measured by the high resolution kaon spectrometer (HKS) [27,28] and high resolution electron spectrometer (HES), respectively. The HKS, which has a Q-Q-D magnet configuration, was constructed and used in the previous $(e,e'K^+)$ experiment, JLab E01-011 [13,14]. The HES, which also has a Q-Q-D magnet configuration, and the SPL were newly constructed for the JLab E05-115 experiment. The HKS detector consists of three layers of time-of-flight (TOF) detectors for a trigger and off-line particle identification (PID), two drift chambers (12 layers in total) for particle tracking and two types of Čerenkov detectors [water ($n = 1.33$) and aerogel ($n = 1.05$)] for both on-line and off-line PID. On the other hand, the HES detector consists of two layers of TOF detectors for the trigger and two drift chambers (16 layers in total) for particle tracking. The important feature of the full magnetic spectrometer system is the momentum resolution of $\Delta p/p \simeq 2.0 \times 10^{-4}$ (FWHM) for both the e' and K^+ spectrometers. This reaction particle resolution results in sub-MeV energy resolution (FWHM) of hypernuclear energy levels. Refer to [14,27,28] for details of the magnets and particle detector systems.

V. MOMENTUM RECONSTRUCTION AND SYSTEMATIC ERROR ON B_Λ

The momentum vectors of an e' and a K^+ were derived by backward transfer matrices which convert positions and angles at the focal plane of each spectrometer to momentum vectors at the target. These are then used to obtain the residual missing mass of the reaction. In our analyses, sixth-order backward transfer matrices were used because they have the minimal complexity to achieve sub-MeV (FWHM) energy resolution. The backward transfer matrices were calibrated [14] with the known masses of Λ and Σ^0 [15] in $p(e,e'K^+)\Lambda$, Σ^0 reactions on a 0.45 g/cm^2 polyethylene target. Systematic errors of the binding and excitation energies were estimated by a full-modeled Monte Carlo simulation which took into account spectrometer acceptance, particle detector resolutions, energy loss, and multiple scattering in all materials (e.g., target, air, detectors). In the simulation, the initial backward transfer matrices were perfect, so they were distorted in order to produce a more realistic simulation, such as peak broadening and shifts in the missing mass spectra. The backward transfer matrices were then optimized by the same code which was used to optimize the matrices with real, measured data. This procedure was tested and repeated with different sets of distorted backward transfer matrices and artificial data. As a result, the differences between the assumed and obtained values in the binding and excitation energies were found to be $\leqslant$0.09 and $\leqslant$0.05 MeV, respectively. Thus, the total systematic errors of the binding energy and the excitation energy, including target thickness uncertainties, were estimated to be 0.11 and 0.05 MeV, respectively.

VI. RESULTS

A. Definition of the differential cross section

The hypernuclear electroproduction cross section can be related to photoproduction by virtual photons [29]. The virtual photon momentum squared, $Q^2 = -q^2 > 0$, is quite small [$Q^2 \simeq 0.01$ (GeV/c)^2, transverse polarization $\epsilon_T \simeq 0.63$] in our experimental geometry. Thus, the (e,e') virtual photon can be approximated by a real photon to obtain the (γ^*, K^+) differential cross section. This results in the following equation:

$$\overline{\left(\frac{d\sigma}{d\Omega_K}\right)} = \frac{\int_{\rm HKS} d\Omega_K \left(\frac{d\sigma}{d\Omega_K}\right)}{\int_{\rm HKS} d\Omega_K} \tag{1}$$

$$= \frac{1}{N_T}\frac{1}{\epsilon^{\rm HES} N_{\gamma^*}}\frac{1}{\epsilon_\kappa}\sum_{i=1}^{N_{\rm HYP}}\frac{1}{\epsilon_i^{\rm HKS}\Delta\Omega_i^{\rm HKS}}. \tag{2}$$

In the above, N_T is the areal density of target nuclei, N_{γ^*} is the number of virtual photons, $N_{\rm HYP}$ is the number of Λ hypernuclei, ϵ's are correction factors including various efficiencies (trigger efficiency, detector efficiency, event selection efficiency, K^+ decay factor, K^+ absorption factor, etc.), and $\Delta\Omega_i^{\rm HKS}$ is the HKS solid angle. The $\Delta\Omega_i^{\rm HKS}$ was calculated event by event, depending on K^+ momentum. We estimated an integral of the virtual photon flux, which is defined in [29], over the HES acceptance with a Monte Carlo technique. The integrated virtual photon flux was obtained as 5.67×10^{-5} [/electron], and it was multiplied by the number of incident electrons on the target to evaluate the N_{γ^*}. The $\Delta\Omega_i^{\rm HKS}$ and some of correction factors were also estimated by Monte Carlo simulations. It is noted that the differential cross section is averaged over the acceptance of our spectrometer system as shown in [14].

B. Missing mass spectrum and peak fitting

Figure 2 shows the Λ binding energy spectrum of $^{10}_{\Lambda}$Be. The target, a 0.056 g/cm^2 ^{10}B foil, was isotopically enriched to a purity of 99.9%. The nuclear masses, 8392.75 and 9324.44 MeV/c^2, for ^{9}Be [30] and ^{10}B [30], respectively, were used to calculate the Λ binding energy. The spectrum of accidental coincidences between an e' and a K^+ was obtained

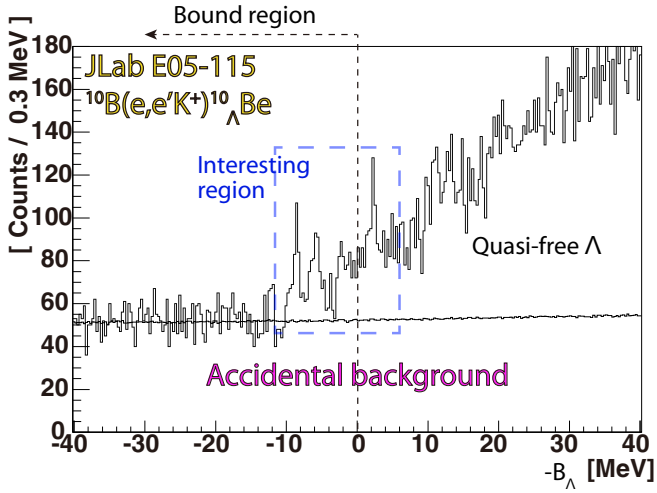

FIG. 2. Binding energy spectrum of $^{10}_{\Lambda}$Be. A distribution of an accidental coincidence between an e' and a K^+ was obtained by the mixed event analysis as described in the text.

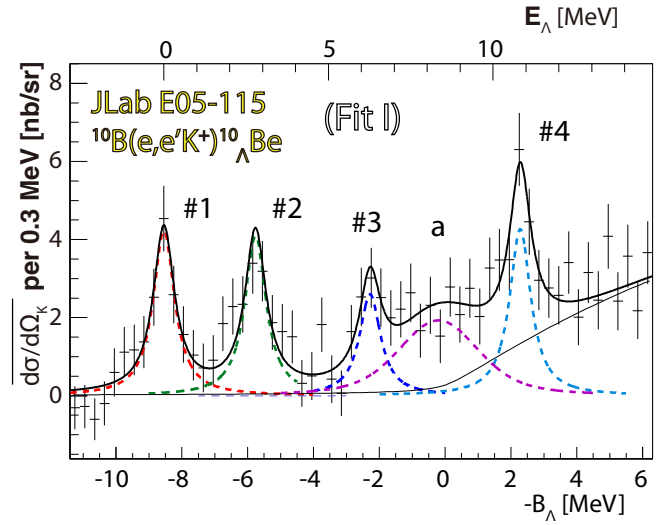

FIG. 3. Binding energy (B_Λ) and excitation energy [$E_\Lambda \equiv -(B_\Lambda - B_\Lambda(\#1))$] spectra for the ^{10}B(e,$e'K^+$)$^{10}_{\Lambda}$Be reaction with a fitting result of Fit I. The ordinate axis is $(\overline{d\sigma/d\Omega_K})$ per 0.3 MeV.

by the mixed event analysis. This analysis reconstructs the missing mass with a random combination of e' and K^+ events in each spectrometer acceptance in an off-line analysis. The method gives the accidental-coincidence spectrum with higher statistics as much as we needed to reduce the effect of statistical uncertainty enough when the accidental-coincidence spectrum was subtracted from the original missing mass spectrum in the further analysis.

The quasifree Λ ($-B_\Lambda \geqslant 0$) spectrum was assumed to be represented by a third-order polynomial function convoluted by a Voigt function (convolution of Lorentz and Gauss functions) having the experimental energy resolution. The accidental coincidence and quasifree Λ spectra were subtracted from the original binding energy spectrum, and a test of statistical significance ($= S/\sqrt{S+N}$) was performed to find peak candidates.

Figure 3 shows the binding energy spectrum with the ordinate axis of $(\overline{d\sigma/d\Omega_K})$, as defined by Eq. (2). A fitting result by Voigt functions for peak candidates with statistical significance of $\geqslant 5\sigma$ are also shown in the figure. The peak candidates are labeled #1, #2, #3, and #4, and are identified as candidates of hypernuclear states.

The enhancements between peaks #3 and #4 are considered to be several states and were included by fitting with a shape having a broader width (indicated as *a* in Fig. 3). The FWHMs of the Voigt functions for peaks of #1–#4 and *a* were found to be 0.78 and 2.87 MeV, respectively. The 0.78 MeV (FWHM) resolution is almost three times better than the measurement of its mirror Λ hypernucleus, $^{10}_{\Lambda}$B measured at KEK (2.2 MeV FWHM) using the (π^+, K^+) reaction [31]. The fitted results are summarized in Table I as Fit I. The statistical error is given in the results.

Figure 4 shows the measured excitation energy levels (Fit I), the theoretical calculations of $^{10}_{\Lambda}$Be [23,32–34], and the experimental results for ^{9}Be [35] and $^{10}_{\Lambda}$B [31]. The differential cross section of each state for the ^{10}B(γ^*, K^+)$^{10}_{\Lambda}$Be reaction relates to that of a spectroscopic factor (C^2S) of the proton pickup reaction from ^{10}B. The C^2S of ^{10}B(e,e'p)^{9}Be are reported in [35], and they are 1.000, 0.985, 0.668, and 1.299 for $J^\pi = 3/2^-, 5/2^-, 7/2^-_1$, and $7/2^-_2$ states in ^{9}Be, respectively. Comparing energy levels and the differential cross sections of hypernuclear states (Table I) with energy levels of ^{9}Be (Fig. 4) and C^2S of ^{10}B(e,e'p)^{9}Be, peaks #1, #2, #3, and #4, respectively, correspond to $J^\pi = 3/2^-, 5/2^-, 7/2^-_1$, and $7/2^-_2$ states in ^{9}Be. In the theoretical predictions of $^{10}_{\Lambda}$Be energy levels shown in Fig. 4, the states of 0^-, 1^- (^{9}Be$[J^\pi; E_x] \otimes j^\Lambda = [1/2^-; 2.78\ \mathrm{MeV}] \otimes s^\Lambda_{1/2}$) and 0^+, 1^+ (^{9}Be$[J^\pi; E_x] \otimes j^\Lambda = [1/2^+; 1.68\ \mathrm{MeV}] \otimes s^\Lambda_{1/2}$) are predicted to be above the $2^-, 3^-$ states (^{9}Be$[J^\pi; E_x] \otimes j^\Lambda = [5/2^-; 2.43\ \mathrm{MeV}] \otimes s^\Lambda_{1/2}$) by about 1 MeV. There might be a possibility that these states are at around 1 MeV above peak #2, assuming peak #2 corresponds to the 2^- and 3^- states. Thus, a fitting with an additional peak function (labeled as *b*) with a width of 0.78 MeV (FWHM) around 1 MeV above peak #2 was also performed, and the fitting result is shown in Table I (labeled as Fit II) and Fig. 5.

A systematic error on the cross section come from uncertainties of trigger efficiency, analysis efficiencies such as tracking and event selection, correction factors such as the solid angle of the spectrometer system and K^+ decay factor, and so on. A square root of the sum of squares of these uncertainties was obtained to be 9%, and it is used as the systematic error on the differential cross section. Obtained differential cross sections of peaks #4 and *a* depend on the assumption of quasifree Λ distribution in the fitting. We tested usages of lower-order polynomial functions (first and second orders) for the quasifree Λ events in order to estimate additional systematic errors for peaks #4 and *a*. As a result, the differential cross sections for peaks #4 and *a* were changed by $\leqslant +5\%$ and $\leqslant +41\%$, respectively, although the others were not changed within the statistical errors. Therefore, the systematic errors on the differential cross sections for peaks #4 and *a* were estimated to be $(+10\%/-9\%)$ and $(+42\%/-9\%)$, respectively. It is noted that in the test, the obtained peak means

TABLE I. Binding energies (B_Λ), excitation energies [$E_\Lambda \equiv -(B_\Lambda - B_\Lambda(\#1))$] and differential cross sections for ^{10}B$(\gamma^*, K^+)\,^{10}_{\Lambda}$Be. The error is statistical. The systematic errors on B_Λ and E_Λ are 0.11 and 0.05 MeV, respectively. The systematic errors on the differential cross sections are ±9% for #1,#2,#3,b; (+10%/−9%) for #4; and (+42%/−9%) for a.

ID	Fit I			Fit II		
	$-B_\Lambda$ (MeV)	E_Λ (MeV)	$(\overline{\frac{d\sigma}{d\Omega_K}})$ (nb/sr)	$-B_\Lambda$ (MeV)	E_Λ (MeV)	$(\overline{\frac{d\sigma}{d\Omega_K}})$ (nb/sr)
#1	−8.55 ± 0.07	0.0	17.0 ± 0.5	−8.55 ± 0.07	0.0	17.1 ± 0.5
#2	−5.76 ± 0.09	2.78 ± 0.11	16.5 ± 0.5	−5.87 ± 0.18	2.68 ± 0.19	14.5 ± 0.4
#3	−2.28 ± 0.14	6.26 ± 0.16	10.5 ± 0.3	−2.29 ± 0.14	6.26 ± 0.15	10.7 ± 0.3
#4	+2.28 ± 0.07	10.83 ± 0.10	17.2 ± 0.5	+2.29 ± 0.07	10.83 ± 0.10	17.7 ± 0.5
a	−0.20 ± 0.40	8.34 ± 0.41	23.2 ± 0.7	−0.19 ± 0.38	8.36 ± 0.39	20.5 ± 0.6
b				−4.98 ± 0.53	3.57 ± 0.53	4.4 ± 0.1

for all of the peak candidates did not vary within the statistical errors.

VII. DISCUSSION

Peak #1 is identified as the sum of the 1^- and 2^- states (^{9}Be$[J^\pi; E_x] \otimes j^\Lambda = [3/2^-; \text{g.s.}] \otimes s^\Lambda_{1/2}$). The energy spacing between these two states is expected to be less than ∼0.1 MeV according to a γ-ray measurement of the mirror hypernucleus $^{10}_{\Lambda}$B [36] and theoretical calculations [23,33]. The differential cross sections for these states were predicted to be comparable in distorted-wave impulse approximation (DWIA) calculations [37]. We performed a simulation varying the cross-section ratio of 1^- to that of 2^- from 0.5 to 1.5, and also the energy separation between these two states from 0.05 to 0.15 MeV, in order to estimate the ground-state binding energy. As a result of the simulation, the ground-state binding energy would be

$$B^{\text{g.s.}}_\Lambda\left(^{10}_{\Lambda}\text{Be}\right) = B_\Lambda(\#1) + C_1, \tag{3}$$

where $C_1 = 0.05 \pm 0.05$ MeV. Thus,

$$B^{\text{g.s.}}_\Lambda\left(^{10}_{\Lambda}\text{Be}\right) = (8.55 + 0.05) \pm 0.07^{\text{stat.}} \pm (0.11 + 0.05)^{\text{sys.}}\ \text{MeV} \tag{4}$$

$$= 8.60 \pm 0.07^{\text{stat.}} \pm 0.16^{\text{sys.}}\ \text{MeV}. \tag{5}$$

A comparison of the binding energy of $^{10}_{\Lambda}$Be with its isotopic mirror hypernucleus $^{10}_{\Lambda}$B provides information on the ΛN CSB effect. Before comparing the current results with previous measurements, we note that there appears to be a systematic discrepancy between the binding energies obtained from emulsion experiments and those obtained from (π^+, K^+) experiments. This is illustrated in Fig. 6, which shows the binding energy differences between the emulsion experiments [16] and the (π^+, K^+) experiments [2]. The binding energy of $^{10}_{\Lambda}$B was measured by both the emulsion experiment [16] and the (π^+, K^+) experiment [31]. The reported binding energies of $^{10}_{\Lambda}$B obtained by the emulsion experiment and (π^+, K^+) experiment are respectively $8.89 \pm 0.06^{\text{stat.}} \pm 0.04^{\text{sys.}}$ MeV and $8.1 \pm 0.1^{\text{stat.}} \pm 0.5^{\text{sys.}}$ MeV, which are not consistent.

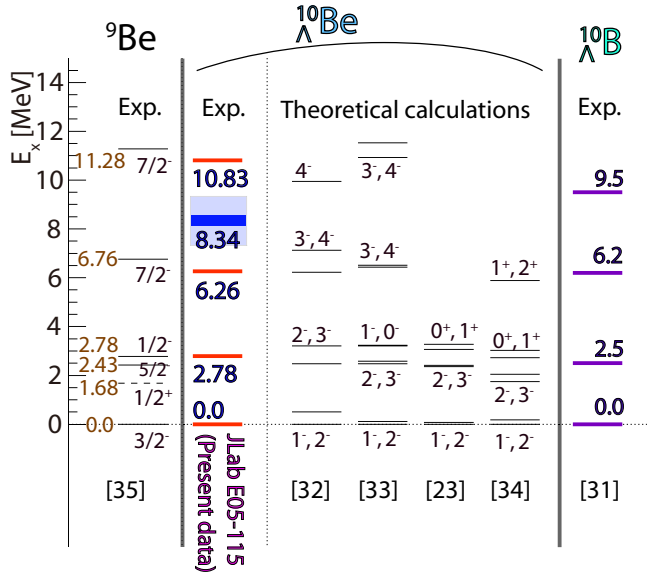

FIG. 4. Obtained energy levels of $^{10}_{\Lambda}$Be (Fit I) compared to those of the theoretical calculations [23,32–34]. The energy levels of ^{9}Be [35] and $^{10}_{\Lambda}$B [31] are shown for comparison as well.

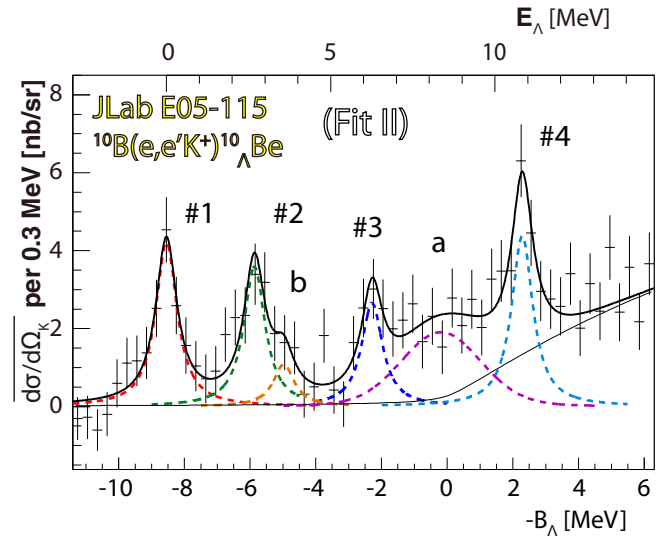

FIG. 5. Binding energy (B_Λ) and excitation energy [$E_\Lambda \equiv -(B_\Lambda - B_\Lambda(\#1))$] spectra for the ^{10}B$(e,e'K^+)\,^{10}_{\Lambda}$Be reaction with a fitting result of Fit II. The ordinate axis is $(\overline{d\sigma/d\Omega_K})$ per 0.3 MeV.

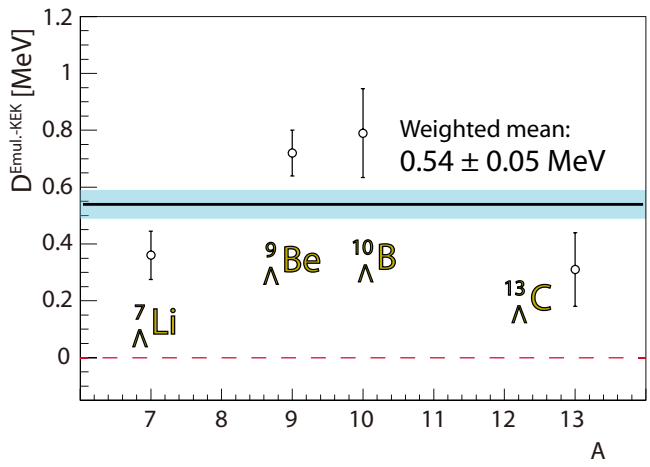

FIG. 6. Binding energy differences of ${}^{7}_{\Lambda}$Li, ${}^{9}_{\Lambda}$Be, ${}^{10}_{\Lambda}$B, and ${}^{13}_{\Lambda}$C between the emulsion experiments [16] and the (π^+,K^+) experiments [2] with the statistical errors. The values of (π^+,K^+) experiments were subtracted from those of the emulsion experiments. The obtained weighted mean was $+0.54 \pm 0.05$ MeV as represented by a solid line. The plots should be on a line of zero (dashed line) if the binding energies measured in the (π^+,K^+) and emulsion experiments are consistent.

In the (π^+,K^+) experiment, however, the binding energy was derived using a reference of binding energy of ${}^{12}_{\Lambda}$C which was measured by the emulsion experiments [16,38]. There are binding energy data of ${}^{7}_{\Lambda}$Li, ${}^{9}_{\Lambda}$Be, ${}^{10}_{\Lambda}$B, and ${}^{13}_{\Lambda}$C by the (π^+,K^+) experiments using the ${}^{12}_{\Lambda}$C reference to be compared with those measured in the emulsion experiments. The binding energy differences of ${}^{7}_{\Lambda}$Li, ${}^{9}_{\Lambda}$Be, ${}^{10}_{\Lambda}$B, and ${}^{13}_{\Lambda}$C between the emulsion experiments [16] and the (π^+,K^+) experiments [2] with the statistical errors are respectively $D_{\text{Emul.}-\text{KEK}} = +0.36 \pm 0.09$, $+0.72 \pm 0.08$, $+0.79 \pm 0.16$, and $+0.31 \pm 0.13$ MeV as shown in Fig. 6. It seems there is a systematic energy difference, and the difference is found to be $D^{\text{fit}}_{\text{Emul.}-\text{KEK}} = +0.54 \pm 0.05$ MeV by the weighted mean of these four points as represented by a solid line in Fig. 6. It indicates that the reported binding energy of ${}^{12}_{\Lambda}$C is shifted by about ($C_2 \equiv$) 0.54 MeV. If the binding energy of ${}^{10}_{\Lambda}$B measured by the (π^+,K^+) experiment is corrected with C_2, it becomes consistent with that of the emulsion experiment within the errors. Since the results from the (π^+,K^+) experiments are all calibrated to the earlier ${}^{12}_{\Lambda}$C binding energy measurement, it is prudent to consider the possibility that they should be recalibrated to the emulsion results for the four hypernuclei shown in Fig. 6.

The ground-state binding energies of ${}^{10}_{\Lambda}$B and ${}^{10}_{\Lambda}$Be to be compared with each other, taking into account the above corrections ($C_{1,2}$), are summarized in Table II. The present result shows that the ground-state binding energy of ${}^{10}_{\Lambda}$Be is shallower than the weighted-mean value of three events reported in the emulsion experiments by 0.51 ± 0.23 MeV, and differences of the ground-state binding energies between ${}^{10}_{\Lambda}$B and ${}^{10}_{\Lambda}$Be were found to be $\Delta B_\Lambda({}^{10}_{\Lambda}\text{B} - {}^{10}_{\Lambda}\text{Be}) = 0.04 \pm 0.12$ MeV (KEK after the C_2 correction and JLab) and 0.29 ± 0.14 MeV (emulsion and JLab). The obtained binding energy would be a considerable constraint for the study of the ΛN CSB interaction in the $A = 10$, $T = 1/2$ isodoublet Λ hypernuclear system since the effect on the binding energy difference among mirror hypernuclei is expected to be a few hundred keV or less [19,23]. For example, the effect of the ΛN CSB interaction on the binding energy difference between ${}^{10}_{\Lambda}$Be and ${}^{10}_{\Lambda}$B is predicted to be only 0.2 MeV by the four-body cluster model with the phenomenological even-state ΛN CSB potential [23].

In the above discussion, the correction of C_2 ($= 0.54$ MeV) was used for the (π^+,K^+) result. The 0.54 MeV shift of the reported binding energy of ${}^{12}_{\Lambda}$C gives a great impact since it was used as a reference of the binding energy measurements for all the (π^+,K^+) experiments in which most energy levels of Λ hypernuclei with $A > 16$ were obtained and used as theoretical inputs for the study of ΛN potential. Therefore, well-calibrated binding energy measurements particularly for the medium to heavy mass region are needed, and only the $(e,e'K^+)$ experiment would be suitable for that purpose at the moment.

Moreover, the 0.54 MeV shift changes a situation of the binding energy difference in the $A = 12$ isotopic mirror Λ hypernuclear system. Previous published results indicate that there is a large binding energy difference between ${}^{12}_{\Lambda}$C and ${}^{12}_{\Lambda}$B as shown in Table II. The large difference of >0.6 MeV is hard to explain theoretically, and is considered to be caused by an unexpectedly large ΛN CSB effect. However, the binding energy difference becomes ΔB_Λ (${}^{12}_{\Lambda}$C $-{}^{12}_{\Lambda}$B) $= -0.23 \pm 0.19$ MeV (emulsion and JLab) if the correction of

TABLE II. Corrected binding energies compared with each other for $A = 10$ and $A = 12$ Λ hypernuclei. The errors are statistical. The systematic errors are 0.16 MeV for ${}^{10}_{\Lambda}$Be (present data), 0.11 MeV for ${}^{12}_{\Lambda}$B (JLab), 0.04 MeV for ${}^{10}_{\Lambda}$Be, ${}^{10}_{\Lambda}$B, ${}^{12}_{\Lambda}$C and ${}^{12}_{\Lambda}$B measured by the emulsion experiments, and 0.50 MeV for ${}^{10}_{\Lambda}$B measured by the (π^+,K^+) experiment at KEK.

Hypernucleus	Experiment	Reported $B^{\text{g.s.}}_\Lambda$ (MeV)	Correction (MeV)	Corrected $B^{\text{g.s.}}_\Lambda$ (MeV)
${}^{10}_{\Lambda}$Be	Present data	8.60 ± 0.07		8.60 ± 0.07
	Emulsion [24,25]	9.11 ± 0.22		9.11 ± 0.22
${}^{10}_{\Lambda}$B	KEK [31]	8.1 ± 0.1	$C_2 = +0.54$	8.64 ± 0.1
	Emulsion [16]	8.89 ± 0.12		8.89 ± 0.12
${}^{12}_{\Lambda}$B	JLab [14]	11.529 ± 0.025		11.529 ± 0.025
	Emulsion [16]	11.37 ± 0.06		11.37 ± 0.06
${}^{12}_{\Lambda}$C	Emulsion [16,38]	10.76 ± 0.19	C_2	11.30 ± 0.19

$C_2 = 0.54$ MeV is applied. It shows that the binding energy difference between isotopic mirror hypernuclei in the $A = 12$ system is less than a few hundred keV as well as that in the $A = 10$ system, implying the effect of ΛN CSB would be small in p-shell Λ hypernuclei as expected in the theoretical prediction [19].

VIII. SUMMARY

This paper reports on a high resolution $(e,e'K^+)$ experiment which obtained for the first time the energy spectrum of the hypernucleus ${}^{10}_{\Lambda}$Be. The experiment, which used a new magnetic spectrometer system, was successfully carried out to obtain hypernuclear structures with an energy resolution of ~0.78 MeV (FWHM) and a systematic error of 0.11 MeV on the binding energy measurement. The Λ binding energy of the first doublet $(1^-, 2^-)$ was obtained to be 8.55 ± 0.07 MeV. The result implies that the ground state is shallower than that reported in the emulsion experiment by about 0.5 MeV, which would provide insight into the study of the CSB effect in the ΛN interaction. In the discussion of the binding energy difference between $A = 10$, $T = 1/2$ isodoublet hypernuclei, a correction of 0.54 MeV on ${}^{12}_{\Lambda}$C which is indicated by the emulsion and (π^+, K^+) experiments was used. The 0.54 MeV correction on ${}^{12}_{\Lambda}$C binding energy makes results in the emulsion and (π^+, K^+) experiments consistent, and supports a small ΛN CSB effect in the $A = 10$ and $A = 12$ hypernuclear systems.

The present result demonstrated that the $(e,e'K^+)$ experiment is able to measure energy levels with a better accuracy in addition to higher resolution than that of the hadron missing mass spectroscopy, and it would be a powerful tool for investigating energy levels of Λ hypernuclei, particularly for the medium to heavy mass region in the future.

ACKNOWLEDGMENTS

We thank the JLab staffs of the physics, accelerator, and engineer divisions for support for the experiment. Also, we thank E. Hiyama, M. Isaka, D. J. Millener, Y. Yamamoto, and T. Motoba for intensive discussions related to their theoretical works. The program at JLab Hall-C is supported by JSPS KAKENHI Grants No. 12002001, No. 15684005, No. 16GS0201, and No. 244123 (Grant-in-Aid for JSPS fellow), JSPS Core-to-Core Program No. 21002, and JSPS Strategic Young Researcher Overseas Visits Program for Accelerating Brain Circulation No. R2201. This work is supported by U.S. Department of Energy Contracts No. DE-AC05-84ER40150, No. DE-AC05-06OR23177, No. DE-FG02-99ER41065, No. DE-FG02-97ER41047, No. DE-AC02-06CH11357, No. DE-FG02-00ER41110, and No. DE-AC02-98CH10886, and US-NSF Contracts No. 013815 and No. 0758095.

[1] M. Danysz and J. Pniewski, Phil. Mag. **44**, 348 (1953).
[2] O. Hashimoto and H. Tamura, Prog. Part. Nucl. Phys. **57**, 564 (2006).
[3] List of proposed experiments, http://j-parc.jp/researcher/Hadron/en/Experiments_e.html
[4] T. R. Saito *et al.*, Nucl. Phys. A **881**, 218 (2012).
[5] A. Esser *et al.*, Phys. Rev. Lett. **114**, 232501 (2015).
[6] T. O. Yamamoto *et al.*, Phys. Rev. Lett. **115**, 222501 (2015).
[7] T. Miyoshi *et al.*, Phys. Rev. Lett. **90**, 232502 (2003).
[8] L. Yuan *et al.*, Phys. Rev. C **73**, 044607 (2006).
[9] M. Iodice *et al.*, Phys. Rev. Lett. **99**, 052501 (2007).
[10] F. Cusanno *et al.*, Phys. Rev. Lett. **103**, 202501 (2009).
[11] F. Cusanno *et al.*, Nucl. Phys. A **835**, 129 (2010).
[12] O. Hashimoto *et al.*, Nucl. Phys. A **835**, 121 (2010).
[13] S. N. Nakamura *et al.*, Phys. Rev. Lett. **110**, 012502 (2013).
[14] L. Tang *et al.*, Phys. Rev. C **90**, 034320 (2014).
[15] K. Nakamura *et al.*, J. Phys. G **37**, 075021 (2010).
[16] D. H. Davis, Nucl. Phys. A **754**, 3c (2005).
[17] B. F. Gibson, A. Goldberg, and M. S. Weiss, Phys. Rev. C **6**, 741 (1972).
[18] A. R. Bodmer and Q. N. Usmani, Phys. Rev. C **31**, 1400 (1985).
[19] A. Gal, Phys. Lett. B **744**, 352 (2015).
[20] A. Nogga, H. Kamada, and W. Glöckle, Phys. Rev. Lett. **88**, 172501 (2002).
[21] E. Hiyama, Y. Yamamoto, T. Motoba, and M. Kamimura, Phys. Rev. C **80**, 054321 (2009).
[22] Y. Akaishi, T. Harada, S. Shinmura, and K. S. Myint, Phys. Rev. Lett. **84**, 3539 (2000).
[23] E. Hiyama and Y. Yamamoto, Prog. Theor. Phys. **128**, 105 (2012).
[24] M. Jurič *et al.*, Nucl. Phys. B **52**, 1 (1973).
[25] T. Cantwell *et al.*, Nucl. Phys. A **236**, 445 (1974).
[26] K. Nakazawa *et al.*, Prog. Theor. Exp. Phys., 033D02 (2015).
[27] T. Gogami *et al.*, Nucl. Instrum. Methods Phys. Res., Sect. A **729**, 816 (2013).
[28] Y. Fujii *et al.*, Nucl. Instrum. Methods Phys. Res., Sect. A **795**, 351 (2015).
[29] M. Sotona and S. Frullani, Prog. Theor. Phys. Suppl. **117**, 151 (1994).
[30] G. Audi, A. H. Wapstra, and C. Thibault, Nucl. Phys. A **729**, 337 (2003).
[31] T. Hasegawa *et al.*, Phys. Rev. C **53**, 1210 (1996).
[32] T. Motoba, P. Bydžovský, M. Sotona, and K. Itonaga, Prog. Theor. Phys. Suppl. **185**, 224 (2010).
[33] D. J. Millener, Nucl. Phys. A **881**, 298 (2012).
[34] M. Isaka *et al.*, Few Body Syst. **54**, 1219 (2013).
[35] D. R. Tilley *et al.*, Nucl. Phys. A **745**, 155 (2004).
[36] H. Tamura *et al.*, Nucl. Phys. A **754**, 58c (2005).
[37] T. Motoba, M. Sotona, and K. Itonaga, Prog. Theor. Phys. Suppl. **117**, 123 (1994).
[38] P. Dluzewski *et al.*, Nucl. Phys. A **484**, 520 (1988).